

Simple Growth and Characterization of α -Sb₂O₄: Evaluation of their Photo-catalytic and Chemical Sensing Applications

¹ASLAM JAMAL, ^{2,3}MOHAMMED MUZIBUR RAHMAN, ^{2,3}SHER BAHADAR KHAN*, ¹MOHAMMED MARGUB ABDULLAH, ¹MOHD FAISAL, ^{2,3}ABDULLAH MUHAMMAD ASIRI, ^{2,3}AFTAB ASLAM PARWAZ KHAN, ⁴KALSOOM AKHTAR

¹Centre for Advanced Materials and Nano-Engineering (CAMNE) and Department of Chemistry, Faculty of Sciences and Arts, Najran University, P. O. Box 1988, Najran, 11001, Kingdom of Saudi Arabia.

²Center of Excellence for Advanced Materials Research (CEAMR), King Abdulaziz University, Jeddah 21589, P.O. Box 80203, Saudi Arabia.

³Chemistry Department, Faculty of Science, King Abdulaziz University, Jeddah 21589, P.O. Box 80203, Saudi Arabia.

⁴Division of Nano Sciences and Department of Chemistry, Ewha Womans University, Seoul 120-750, Korea. drkhanmarwat@gmail.com*

(Received on 23rd July 2012, accepted in revised form 12th November 2012)

Summary: A comprehensive study on the synthesis, characterization and application of antimony oxide (α -Sb₂O₄) has been reported in this paper. Antimony oxide (α -Sb₂O₄) is successfully synthesized by hydrothermal method using antimony chloride and urea as a reducing materials. The morphology of the nanomaterial is investigated by field emission scanning electron microscopy (FE-SEM). Sheet like morphology of α -Sb₂O₄ ranging from 0.2 μ m to 3.0 μ m are found in the FE-SEM images. The detailed structural characterizations are performed by X-ray diffraction (XRD), Fourier transform infrared spectrophotometer (FT-IR), and Raman spectrophotometer respectively. It has been confirmed that the synthesized materials are well-crystalline and pure antimony oxide (α -Sb₂O₄). Optical properties are studied using UV-VIS spectrophotometer, where the direct band-gap of α -Sb₂O₄ is calculated to be 3.26 eV. The photo-catalytic degradation and chemical sensing applications are successfully checked by simple and reliable UV/vis. spectroscopy and I-V methods respectively.

Keywords: Antimony oxide, Structural properties, Optical properties, Photo-catalytic degradation, Chloroform sensing

Introduction

Semiconducting materials show potential applications in sensor technology [1-16], electronic devices, solar energy conversion [17], and in field emitter [18] due to their excellent optical and electrical properties. Being a member of V-VI group of semiconductor family, antimony oxide demonstrates outstanding performances. Mainly, three different kinds of antimony oxides Sb₂O₃ [19], Sb₂O₄ [20], and Sb₂O₅ [21] are known. Out of these three metal oxides, Sb₂O₄ is least studied. Two polymorphs of antimony oxide (Sb₂O₄) orthorhombic α -Sb₂O₄ and monoclinic β -Sb₂O₄ are reported [20] and for the present study, α -Sb₂O₄ has been selected.

Synthesis of nano-sized materials has attracted the attention of researchers due to its novel properties, which depends on their characteristics like size, shape, and crystallinity [21, 22]. Out of various synthesis processes, the preparation of nano-sized materials using hydrothermal method is easy, cost-reducing and efficient [23]. In principle, nano-structured antimony oxides can be synthesized by various methods like vapor-solid route [24], hydrothermal [25], vapor condensation [26], sol-gel [27], X-ray radiation-oxidization route [28] and gas condensation [29]. For the present study, low

dimensional α -Sb₂O₄ was grown by hydrothermal method.

In general, the antimony oxide is used as conductive materials, flame-retardant synergist in polymers, high-efficiency dye and pigment, paints, adhesives and industrial coating materials [30]. It is also used in fireworks, ceramics, and lead storage batteries and as enamels for plastics. α -Sb₂O₄ collectively with other oxide has been extensively used as a catalyst for the oxidation of propane to acrylonitrile.

Because of numerous pollutants, water, soil and environment pollutions are major issue globally. Researchers have reported several kind of photo-catalytic degradation of organic pollutants [3-10]. Metal oxides are strong decoloring agent. It plays effective role in the treatment of waste water effluents. The degradation of acridine orange (AO) using metal oxides (MO_x) nanostructures, in the presence of radiation sources illumination has become a promising technology for the removal of heterogeneous and homogeneous dye and pigment as contaminants from wastewater [3-10]. Therefore, the application of antimony oxide by photocatalytic

*To whom all correspondence should be addressed.

degradation using acridine orange dyes have been tested and reported in this paper.

Chloroform is one of the essential organic compounds. Its vapor causes cardiac or respiratory arrest and depresses the central nervous system [10]. In the present work, we have studied the chloroform sensing on antimony oxide and thus observed the detection and quantification of chloroform on α -Sb₂O₄. In addition to photo-catalytic degradation and sensing, the synthesized α -Sb₂O₄ has been characterized in detail in terms of their morphological, structural and optical properties.

Results and Discussion

To check the crystallinity and crystal structure of as-synthesized α -Sb₂O₄ powder, X-ray diffractometry (XRD) analysis was carried out with monochromated CuK α 1 radiation (45.0 KV, 30.0 mA), scanned in step size of 0.02° for the angular range 15-60° of 2 θ . Fig. 1(a) shows the recorded XRD pattern of as synthesized α -Sb₂O₄. The general aspect of this XRD patterns (Fig. 1(a)), in particular, the presence of strong and sharp peaks and the absence of diffraction halo, indicate the presence of crystalline phase only and show the absence of amorphous or crystalline-amorphous phase formation. The obtained values of d-spacing are in good agreement with that of reported values [20], confirming that as-synthesized α -Sb₂O₄ has orthorhombic structure. The diffraction lines (Fig. 1(a)) have been indexed with the help of reported values [7]. The most intense peak correspond to (112) plane. This shows that the preferential orientations of crystalline grains are along this plane. By using Debye-Scherrer formula, the crystallite size associated with this peak was found to be 35.0 nm.

Fig. 1(b-c) demonstrates the FE-SEM images of antimony oxide (α -Sb₂O₄) at low and high magnification, respectively. From the fig, it has been observed that all particles are not uniform in shape, while most of them represent a sheet like morphology (Fig. 1(c)). The average length of sheets lies within the range 0.2 μ m to 3.0 μ m, respectively. The energy dispersive spectroscopy (EDS) spectrum (Fig. 1(d)) revealed the composition of antimony oxide. The peak indicates the presence of antimony (Sb) and oxygen (O). The atomic percentage of Sb and O were found in 31.68 and 68.32% respectively.

UV/visible spectroscopy is a process in which the outer electrons of atoms or molecules absorb radiant energy and undergo transitions to high energy levels. In this process, the spectrum obtained due to optical absorption can be analyzed to get the energy band-gap of the material. The optical absorption measurement was carried out at ambient conditions. From the spectrum (Fig. 2(a)), it has been observed that the lower cut off wavelength for the as-synthesized α -Sb₂O₄ is around 368.0 nm. Also, the spectrum doesn't show any absorption peak in the wavelength range 400-500 nm. Hence, the titled compound may be useful for the fabrication of NLO (Non-linear optical) devices in this wavelength region, as the absence of absorption peaks is the main requirement for the materials to show NLO properties. To know the optical band gap for the as-grown α -Sb₂O₄, a plot of $(\alpha h\nu)^2$ versus incident photon energy ($h\nu$) has been shown in Fig. 2(b). The direct band gap energy was evaluated by extrapolating the straight-line portion of the plot " $(\alpha h\nu)^2$ " vs " $h\nu$ " to zero absorption coefficient value. From the graph (Fig. 2(b)), the value of band gap was found to be \sim 3.26 eV.

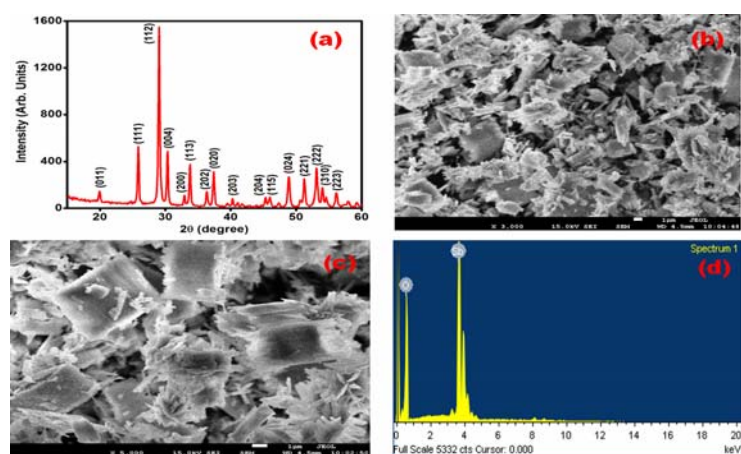


Fig. 1: (a) XRD pattern, (b)-(c) FE-SEM images and (d) EDS of dried antimony oxide grown by hydrothermal process.

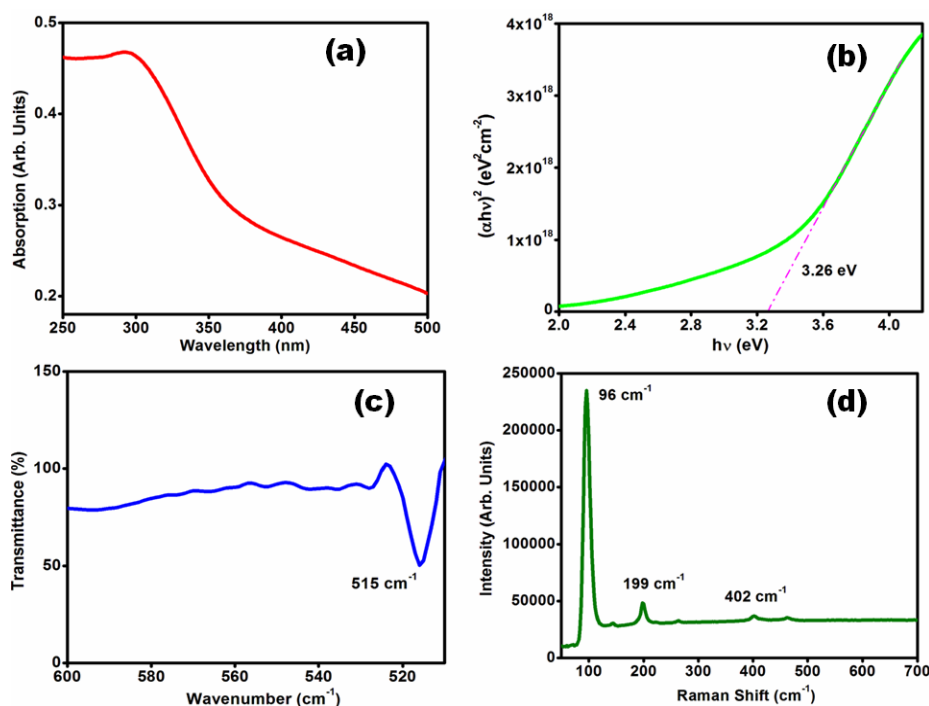


Fig. 2: (A) UV/visible spectrum, (b) Band gap energy graph (c) FT-IR spectra and (d) Raman spectroscopy of as-synthesized α - Sb_2O_4 .

Fig. 2(b) shows the typical FT-IR spectra of the as-grown α - Sb_2O_4 . The figure shows an absorption band at 515cm^{-1} . This is the characteristic peak for the O-Sb-O stretching vibration in α - Sb_2O_4 . Further, the high intensity of the absorption band at 515cm^{-1} confirms that the α - Sb_2O_4 have been grown in high density. Raman spectroscopy is a promising technique for the structure details of materials. This technique has been extensively used to discriminate different structures since it directly probes structures and bonds by its vibrational spectrum. Fig. 2(C) shows the Raman spectrum of as-synthesized α - Sb_2O_4 . This spectrum contains three sharp Raman lines at 96, 199, and 402cm^{-1} . These observed Raman lines are due to the vibrational modes of O-Sb-O and Sb-O-Sb, respectively [31].

Applications

Photo Catalytic Degradation

The performance of α - Sb_2O_4 as photocatalyst was evaluated by degrading acridine orange and the extent of degradation was monitored by UV-vis. Spectrophotometer [3-10]. Fig. 3(A) shows the gradual decreasing in absorption spectra for the degradation as a function of photo-irradiation time. It is observed that the irradiation of an aqueous

suspension of AO dye in the presence of α - Sb_2O_4 leads to decrease in absorption spectra at 491nm . The absorbance spectra at 491nm is significantly decreased with increasing in exposure time and gradually decrease until 170.0 minutes which concludes that the AO dye has de-colorization property with micro α - Sb_2O_4 close to 52.1%. The decrease in absorption spectra *versus* irradiation time for the AO in the presence and absence of α - Sb_2O_4 is shown in the Fig. 3(B). Fig. 3(C) shows a plot for the % degradation vs. irradiation time (min) for the oxygen saturated aqueous suspension of α - Sb_2O_4 containing AO. It shows that around 52.1% degradation of the AO dye takes place after 170 min of irradiation in the presence of catalytic of α - Sb_2O_4 . The mechanism of semiconductor photocatalysis has widely been studied. Generally when a photon of energy equal to or greater than its band-gap width irradiate α - Sb_2O_4 , it leads to the formation of electron/hole (e^-/h^+) pairs with free electrons produced in the empty conduction band (e^-_{CB}) leaving behind an electron vacancy or "hole" in the valence band (h^+_{VB}). If charge separation is maintained, the electron and hole migrate to the catalyst surface where they participate in redox reactions. Specially, h^+_{VB} may react with surface-bound H_2O or OH^- to produce the hydroxyl radical and e^-_{CB} is picked up by oxygen to generate superoxide radical anion [3-10].

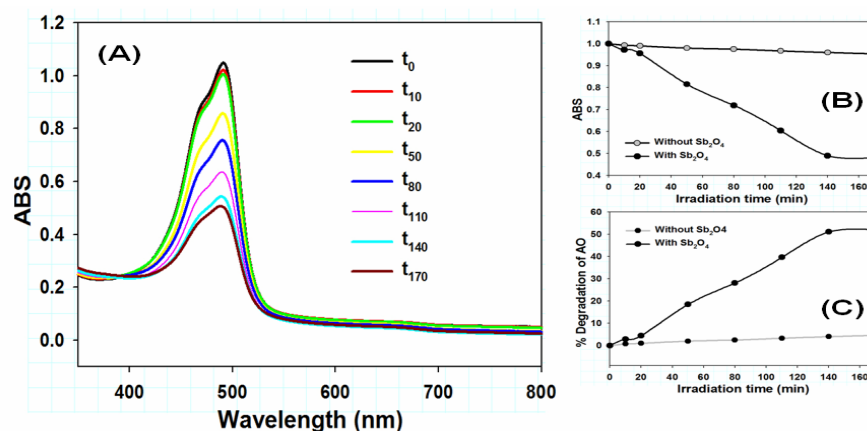


Fig. 3: (A) Absorption spectra, (B) comparative absorbance, and (C) % degradation of AO with dried antimony oxide in 170 min.

The hydroxyl radicals (OH^\cdot) and superoxide radical anions ($O_2^{\cdot-}$) show as a primary oxidizing species in the photocatalytic processes and contribute to the oxidation process by attacking the dye molecules and would result in the bleaching of the AO dye. The absorption of light by the AO dye, can lead to charge injection from the excited state of the dye to the conduction band of the semiconductor. However, the appropriate content of oxygen vacancies can trap either one or two electrons, resulting in the holes free to diffuse to the semiconductor surface where oxidation of organic species can occur. The decrease in electron density within the metal oxides leads to an increase in the hydroxyl group acidity, which in turn improves the photocatalytic activity of $\alpha-Sb_2O_4$. By these phenomena, the more oxygen vacancies will improve the photocatalytic activities of photocatalysts greatly.

Chloroform Sensing

The antimony oxides $\alpha-Sb_2O_4$ was employed for the detection of chloroform in solution phase [1-16]. The thin film of oxides on silver electrode (surface area, 0.0216 cm^2) were made by mixing ethyl cellulose and butyl carbitol acetate properly and embedded on the electrode surface by physisorption method at room temperature [32-38]. The fabricated electrode was kept in the oven at 60.0°C for 6 hours to dry the film completely. Palladium (PdE) and silver (AgE) electrodes were used as counter electrode and working electrode, respectively [37, 38]. I-V technique was followed to measure the variation in current with each injection ($100.0 \mu\text{L}$) of chemical solution in the 10.0 mL solution [32-36]. I-V response of the sensor with and without $\alpha-Sb_2O_4$

thin film as a function of time for the chloroform is presented in Fig. 4(A) and Fig. 4(B). The time delaying for electrometer was kept 1.0 second. The concentration of chloroform was varied from $12.0 \mu\text{M}$ to 60.0 mM by adding de-ionized water in different proportions. A significant increase in the current value with applied potential is clearly demonstrated. The gray-solid and dark-solid dotted curves (Fig. 4(B)) indicate the response of the film before and after injecting $100.0 \mu\text{L}$ chemicals in bulk solution. Each I-V response to varying concentration of chemicals from $12.0 \mu\text{M}$ to 1.2 mM on thin antimony oxide ($\alpha-Sb_2O_4$) coatings for 1.0 s (delay of time) is presented in the Fig. 4(C). It shows current of $\alpha-Sb_2O_4$ as a function of target concentration at room temperature. It is observed that at lower to higher concentration of target compound, the current increases gradually. Furthermore, a wide range ($12.0 \mu\text{M}$ to 1.2 mM) of chloroform concentration was chosen to study the possible detection limit. The calibration curve was plotted from the variation of chloroform concentration, which is shown in the Fig. 4(D) [1-16]. The sensitivity was calculated from the calibration curve, which is $1.154 \mu\text{Acm}^{-2}\text{mM}^{-1}$. The linear dynamic range of this sensor exhibits from $12.0 \mu\text{M}$ to 1.2 mM and the detection limit was found $\sim 10.0 \mu\text{M}$.

Experimental

Materials

Analytical grade antimony chloride, urea, ammonium hydroxide, acridine orange and chloroform were purchased from Sigma-Aldrich Company and were used as received.

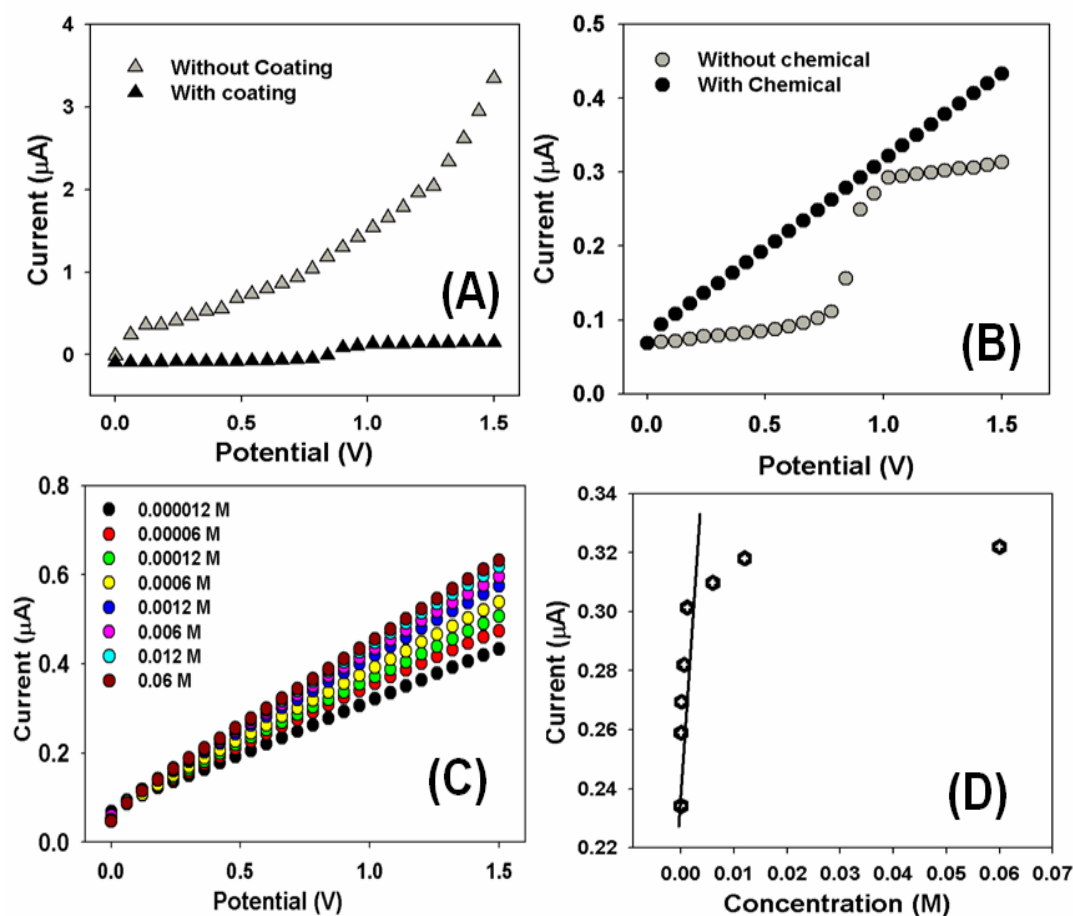


Fig. 4: I-V responses (A) with and without nanomaterials coating on AgE substrate, (B) with and without chloroform, (C) with various concentrations of chloroform, and (D) calibration curve for the detection of chloroform with dried $\alpha\text{-Sb}_2\text{O}_4$.

Synthesis of $\alpha\text{-Sb}_2\text{O}_4$

For the synthesis of antimony oxide, the solutions were prepared by adding antimony chloride (0.1 M, 50.0 mL) and urea (0.1 M, 50.0 mL) in double distilled water in equimolecular proportion. The pH 10.5 was adjusted by adding drop wise ammonium hydroxide to the solution. The solution was mixed using magnetic stirrer on hot-plate. The as-prepared solution was then transferred to a Teflon auto-clave. This autoclave was further placed at the centre of the hydrothermal bomb and heated at 150 $^{\circ}\text{C}$ for 17 hours. After this period, the solution was allowed to cool to room temperature. The white precipitates obtained from this solution were then washed with acetone for two times. The acetone washed precipitates were dried at room temperature. To remove the possible impurities and contamination,

the as-grown material was annealed at 200.0 $^{\circ}\text{C}$ for 2 hours.

Characterization

The structural and morphological analysis of the as-grown $\alpha\text{-Sb}_2\text{O}_4$ were done by using powder X-ray diffraction (XRD) and field emission scanning electron microscopy (FE-SEM), respectively. Energy dispersive spectroscopy (EDS) attached with FE-SEM was used to identify the composition of as-synthesized $\alpha\text{-Sb}_2\text{O}_4$. The optical absorption measurements of $\alpha\text{-Sb}_2\text{O}_4$ have been recorded at room temperature with the help of UV-vis. NIR spectrophotometer (Perkin Elmer-Lambda 950-UV-visible spectrometer). Fourier transforms infrared (FT-IR; Perkin Elmer) spectrum was recorded by making pellet with KBr. Raman-scattering spectrum

was measured at room temperature with the Ar⁺ laser line (λ : 513.4 nm) as an excitation source.

Photo-Catalytic Experiments

For its photo-catalytic activity, photo-degradation of acridine orange (AO) 0.03 mM was carried out with UV light source (250 W) in 250 ml beaker with continuous purging of oxygen. Samples (5.0 ml) were collected at regular interval; centrifuge and change in absorbance were analyzed with the help of Perkin Elmer-Lambda 950-UV-visible spectrometer.

Fabrication of Chemical Sensor

The chemical sensing of α -Sb₂O₄ electrodes have been primarily investigated by I-V technique. A cell was made by using α -Sb₂O₄ coated silver electrode (AgE) as a working electrode and palladium (PdE) wire as a counter electrode. The electrodes were dipped in 10.0 mL phosphate buffer solution of 0.1 M concentration throughout the investigation. Chloroform solution, diluted at different concentrations in de-ionized (DI) water was used as a target chemical. The sensitivity of α -Sb₂O₄ was calculated from the calibration plot by taking the ratio of voltage versus current. Electrometer was used as a voltage source for I-V measurement in simple two electrode systems.

Conclusion

The antimony oxide (α -Sb₂O₄) was successfully synthesized by hydrothermal technique using SbCl₃ and urea in alkaline medium. The composition and detail structural characterizations were done using FE-SEM, EDS, XRD, UV/vis., FT-IR, and Raman spectroscopy. The photo-catalytic activity of the synthesized α -Sb₂O₄ was evaluated by degradation of acridine orange (AO) which degraded almost 52.1% in 170.0 minutes. The analytical performances of the fabricated chloroform sensor demonstrated good sensitivity (1.154 μ Acm⁻²mM⁻¹), lower-detection limit (~10.0 μ M), large-linear dynamic range (12.0 μ M to 1.2 mM) with good linearity (R = 0.8457) in short response time (10.0 sec). This new and novel contribution is commenced an innovative method for proficient chloroform chemical sensor progress for environmental and health care fields.

Acknowledgement

Center of Excellence for Advanced Materials Research (CEAMR), King Abdulaziz

University, Jeddah, Saudi Arabia is highly acknowledged. Authors are also thankful to the deanship of scientific research, Najran University, Najran, Kingdom of Saudi Arabia for financial support.

References

1. M. M. Rahman, S. B. Khan, M. Faisal, A. M. Asiri and K. A. Alamry, *Sensors and Actuators B: Chemical*, **932**, 171 (2012).
2. M. M. Rahman, S. B. Khan, M. Faisal, A. M. Asiri and M. A. Tariq, *Electrochimica Acta*, **75**, 164 (2012).
3. M. M. Rahman, S. B. Khan, M. Faisal, M. A. Rub, A. O. Al-Youbi and A. M. Asiri, *Talanta*, **99**, 924 (2012).
4. S. B. Khan, M. Faisal, M. M. Rahman and A. Jamal, *Science of Total Environment*, **409**, 2987 (2011).
5. M. M. Rahman, A. Jamal, S. B. Khan and M. Faisal, *Journal of Nanoparticle Research*, **13**, 3789 (2011).
6. S. B. Khan, M. Faisal, M. M. Rahman and A. Jamal, *Talanta*, **85**, 943 (2011).
7. M. Faisal, S. B. Khan, M. M. Rahman and A. Jamal, *Journal of Material Science and Technology*, **27**, 594 (2011).
8. A. Jamal, M. M. Rahman, M. Faisal and S. B. Khan, *Material Science Applications*, **2**, 676 (2011).
9. M. Faisal, S. B. Khan, M. M. Rahman and A. Jamal, *Chemical Engineering Journal*, **173**, 178 (2011).
10. M. Faisal, S. B. Khan, M. M. Rahman and A. Jamal, *Applied Surface Science*, **258**, 672 (2011).
11. M. M. Rahman, A. Jamal, S. B. Khan and M. Faisal, *Journal of Physical Chemistry C*, **115**, 9503 (2011).
12. M. M. Rahman, A. Jamal, S. B. Khan and M. Faisal, *ACS Applied Material Interfaces*, **3**, 1346 (2011).
13. M. Faisal, S. B. Khan, M. M. Rahman, A. Jamal and A. Umar, *Material Letters*, **65**, 1400 (2011).
14. M. M. Rahman, A. Jamal, S. B. Khan and M. Faisal, *Biosensing and Bioelectron*, **28**, 127 (2011).
15. M. M. Rahman, A. Jamal, S. B. Khan and M. Faisal, *Superlattice Microstructure*, **50**, 369 (2011).
16. M. M. Rahman, S. B. Khan, A. Jamal, M. Faisal and A. M. Asiri, *Sensing and Transduction Journal*, **134**, 32 (2011).
17. M. Law, L. Greene, J. C. Johnson, R. Saykally and P. Yang, *Nature Matter*, **4**, 455 (2005).

18. H. Jiang, J. Hu, F. Gu and C. Li, *Nanotechnology*, **20**, 055706 (2009).
19. Z. T. Deng, D. Chen, F. Q. Tang, X. W. Meng, J. Ren and L. Zhang, *Journal of Physical Chemistry C*, **111**, 5325 (2007).
20. Z. J. Zhang and X. Y. Chen, *Journal of Physical and Chemical Solid*, **70**, 1121 (2009).
21. L. Guo, Z. Wu, T. Liu, W. Wang and H. Zhu, *Chemistry and Physics Letters*, **318**, 49 (2002).
22. H. Gleiter, *Progress in Material Science*, **33**, 223 (1989).
23. C. R. Wang, K. B. Tang, Q. Yang, S. H. Lu, G. E. Zhou and F. Q. Li, *Journal of Crystal Growth*, **226**, 175 (2001).
24. C. H. Ye, G. W. Men and L. D. Zhang, *Chemical Physics*, **363**, 34 (2002).
25. J. R. Zhang and L. Gao, *Material Chemistry*, **87**, 10 (2004).
26. D. W. Zeng, C. S. Xie and B. L. Zhu, *Material Letters*, **58**, 312 (2004).
27. K. H. Jo and K. H. Yoon, *Material Research Bulletin*, **24**, 1 (1989).
28. Y. P. Liu, Y. H. Zhang, M. W. Zhang, W. H. Zhang and Y. T. Qian, *Materials Science Engineering B*, **49**, 42 (1997).
29. Z. L. Zhang, L. Guo and W. D. Wang, *Journal of Material Research*, **16**, 803 (2001).
30. K. Ozawa, Y. Sakka and A. Amamo, *Journal of Material Research*, **13**, 830 (1998).
31. G. Ren, C. Wang, J. Xia, J. Liu and H. Zhong, *Material Letters*, **63**, 605 (2009).
32. S. B. Khan, M. M. Rahman, K. Akhtar, A. M. Asiri, J. C. Seo and H. Han, *International Journal of Electrochemical Science*, **7**, 4030 (2012).
33. M. M. Rahman, A. Jamal, S. B. Khan, M. Faisal and A. M. Asiri, *Microchimica Acta*, **178**, 99 (2012).
34. M. M. Rahman, A. Jamal, S. B. Khan, M. Faisal, A. M. Asiri, *Talanta*, **95**, 18 (2012).
35. M. Faisal, S. B. Khan, M. M. Rahman, A. Jamal, A. M. Asiri and M. M. Abdullah, *Applied Surface Science*, **258**, 7515 (2012).
36. M. M. Rahman, A. Jamal, S. B. Khan, M. Faisal and A. M. Asiri, *Chemical Engineering Journal*, **192**, 122 (2012).
37. S. R. Lee, M. M. Rahman, M. Ishida and K. Sawada, *Biosensors and Bioelectronics*, **24**, 1877 (2009).
38. S. R. Lee, M. M. Rahman, M. Ishida and K. Sawada, *Trends in Analytical Chemistry*, **28**, 196 (2009).